Improvements of the hydrological processes of the Town Energy Balance Model (TEB-Veg, SURFEX v7.3) for urban modelling and impact assessment

Xenia Stavropulos-Laffaille[1], Katia Chancibault[1], Jean-Marc Brun[1], Aude Lemonsu[2], Valery Masson[2], Aaron Boone[2], Hervé Andrieu[1]

[1]IFSTTAR, GERS, EE, F-44344 Bouguenais, France
[2]CNRM UMR 3589, Météo-France/CNRS, Toulouse, 31057 Toulouse CEDEX 1, France

Correspondence to: Xenia Stavropulos-Laffaille (xenia.laffaille@ifsttar.fr)

Abstract. Climate change and demographic pressure are common issues to be considered when conducting urban planning. Local authorities and stakeholders have therefore opted for more nature-based adaptation strategies, which are especially suitable to influence both hydrological and energy processes. Assessing the multiple benefits of such strategies on the urban microclimate thus requires effective numerical tools. This paper presents recent developments of the water budget in the TEB-Veg model (SURFEX v7.3), which allows for a better representation of the hydrological processes of urban subsoil. This new hydrological module has been called TEB-Hydro. The developments studied concern the introduction of subsoil underneath built surfaces, and the processes of: horizontally rebalancing intra-mesh soil moisture, draining soil water via the sewer network, and limiting deep drainage in the aim of achieving a more realistic base flow pattern in the sewer system. A sensitivity analysis is then performed in order to identify the hydrological parameters required for model calibration. The new TEB-Hydro model is evaluated on two small residential catchments in Nantes (France) by comparing simulated sewer discharges to observation findings. In both cases, the model tends to overestimate total sewer discharge and performs better under wet climate conditions, with a KGE statistical criterion greater than 0.80 vs. roughly 0.60 under drier weather conditions. Yet these findings remain encouraging since the same set of model parameters are identified for both catchments, irrespective of meteorological and local physical conditions. This approach opens opportunities to apply the model at the city scale with respect to projections of climate and demographic changes.

1. Introduction

Urbanisation is the predominant trend in today's world. Cities consume space and energy, generate pollution and nuisances, and are vulnerable to natural or manmade hazards, such as floods and urban heat islands (hereafter denoted UHI), that climate change is likely to exacerbate (EEA, 2012).

The adaptation of cities to global changes (climate change and demographic pressures) has become a major challenge in the field of planning policy. The use of nature-based solutions (hereafter NBS), such as green and blue infrastructure, has been

approved as part of sustainable urban development (Sustainable Urban Drainage Systems, water and pollution source control, insulation of buildings) and is therefore recommended (Hamel *et al.*, 2013; EC, 2015). However, evaluating such adaptation and mitigation strategies requires conducting impact studies capable of assessing the various services these solutions can offer along with their interactions (energy, thermal comfort, water, landscaping, etc.) (Bach *et al.*, 2014). As

5 regards hydro-microclimatic patterns, the processes of evapotranspiration (or latent heat flux) constitute an increasingly significant portion of both the urban water and energy budgets. For modelling purposes, evapotranspiration is thus a key element since it affects the water and energy budgets (Mitchell *et al.*, 2008).

Despite the increased interest in urban hydrology over recent years (Fletcher *et al.*, 2013; Hamel *et al.*, 2013; Shirmer *et al.*, 2013; Salvadore *et al.*, 2015), the various water- and energy-related processes are still rarely addressed with the same level

10 of detail, and the coupling between them is often oversimplified.

In the past, the emphasis on the urban water cycle was directed at the design of urban drainage systems and their operations under extreme events (flooding, low water level). Hydraulic models have thus been used to analyse rainfall-runoff patterns during rain events when evapotranspiration is not a major concern (Berthier *et al.*, 2006; Fletcher *et al.*, 2013). In recent decades however, a more decentralized urban water management system has necessitated impact studies that focus on the

15 urban water cycle as a whole. Consequently, urban hydrological models are being more heavily promoted, even though they still simplify or neglect the energy balance. Evapotranspiration is therefore often calculated from a reference value of potential evapotranspiration, which takes into account soil moisture conditions and sometimes vegetation (Rodriguez *et al.*, 2008; Rossman, 2010; DHI, 2001). At the local level, atmospheric demand is typically not considered a limiting factor for evapotranspiration, and a direct interaction rarely exists between the water balance and the energy balance. In their state-of-

20 the-art paper, Fletcher *et al.* (2013) noted that evapotranspiration in urban areas remains relatively poorly explored.

Unlike hydrological models, the urban micro-climate models (Masson, 2000; Musy *et al.*, 2015; Gros *et al.*, 2016) provide a detailed solution of energy and radiative budgets, while the water balance has been simplified, which can lead to an alteration of the modelled latent heat fluxes (Grimmond *et al.*, 2011). Malys *et al.* (2016) used such a model to evaluate the mitigation effects of vegetation on UHI. Soil moisture however is not considered as a limiting factor, hence potentially

25 leading to an overestimation of the cooling abilities of plants, especially under hot climate conditions. For example, the Town Energy Balance Scheme (TEB) described by Masson (2000) is a mesoscale surface scheme dedicated to the urban environment. The urban environment is presented in a simplified manner by means of the street canyon approach (Oke, 1987), which averages the characteristics of urban covers and morphology (building height, construction materials, canyon aspect ratio, street orientation) inside one grid mesh. This approach initially resolves detailed energy and radiative budgets of

30 built-up areas (buildings and roads), while the hydrological part is presented more simply, i.e.: i) artificial surfaces (buildings and roads) are completely impervious; and ii) water exchanges are thus only taken into account between the surface and the atmosphere. Lemonsu *et al.* (2007) then introduced the rainfall interception capacities of built-up surfaces and integrated water infiltration through artificial surfaces, like roads, pavements and parking lots, into TEB in order to implement more realistic hydrological processes. Using the ISBA-DF model (Interaction Soil-Biosphere-Atmosphere - explicit vertical

diffusion) (Boone *et al.*, 2000) as part of the urban fabric, by integrating vegetated surfaces inside the street canyon, the TEB model has evolved into TEB-Veg (Lemonsu *et al.*, 2012). Interactions within the radiative, energy and water balances between natural and artificial surfaces are now considered. Nevertheless, even if a detailed water balance for the subsoil of natural surfaces is calculated, the water processes occurring in the subsoil of artificial surfaces and their interactions with the

5   surface are still neglected.

The objective of this study is to develop a complete urban hydro-microclimate model, hereafter called TEB-Hydro, by integrating the subsoil under built-up surfaces and hydrological soil-surface interactions into the existing TEB-Veg model. This step will allow treating the energy and water budgets at the same level of detail, which is critical to the impact assessment of NBSs at a city scale. First, the model concept will be described. Since the energy and radiation components of

10   the model have not changed, as fully described in Masson (2000) and Lemonsu *et al.* (2012), the focus is placed on the model's hydrological component and recent model developments. Next, the experimental sites and observation data will be presented. The model evaluation will then be laid out in Section 4 in analysing the simulations performed by the new model version.

2. Description of the TEB-Hydro hydrological model

15   TEB-Hydro is an evolution of TEB-Veg, with SURFEX v7.3 (Lemonsu *et al.*, 2012), and was developed on the SURFEX modelling platform (Masson *et al.*, 2013). Like TEB-Veg, TEB-Hydro is based on a regular grid mesh and can be run either coupled with other meteorological models or in offline mode forced by observed atmospheric data. It combines two surface schemes, TEB (Masson, 2000) and ISBA-DF (Boone *et al.*, 2000), both of which run on an integrated tiling approach and describe energy and water exchanges between the urban and natural subsoils, the surface and atmosphere, respectively. The

20   urban environment is represented by three compartments, such as buildings (roofs and walls), roads (streets, pavements and parking), and gardens. This section will present the new model developments based on the existing TEB-Veg model version. A general description of the hydrological processes will be laid out first, followed by a discussion of the new developments dedicated to hydrological processes in the urban subsoil (Fig. 1).

2.1 General principles of hydrological processes

25   Interactions between the energy balance (Eq. 1) and water balance (Eq. 2) are established via the explicit resolution of the evapotranspiration term (Eq. 3):

$$Q^* + Q_F = Q_H + Q_E + \Delta Q_S + \Delta Q_A \quad [W\ m^{-2}] \tag{1}$$

$$P + I = E + R + D + \Delta W \quad [kg\ m^{-2}\ s^{-1}] \tag{2}$$

$$Q_E = \frac{E}{L_V} \quad [W\ m^{-2}] \tag{3}$$

where Q^* is the net all-wave radiation, Q_F the anthropogenic heat flux, Q_H the sensible heat flux, Q_E the latent heat flux, ΔQ_S the heat flux storage, ΔQ_A the net advection heat flux, P the total precipitation, I the water generated from anthropogenic activities (irrigation), E the evapotranspiration, R the total runoff, D the deep drainage, ΔW the variation in water storage both on the surface and in the ground during the simulation period, and lastly L_v the latent heat of vaporisation (-).

2.1.1 Evapotranspiration

The evaporation is calculated for each surface type E_* (Fig. 1). For built-up surfaces, this value depends on both the surface specific humidity at saturation and the air humidity (inside the canyon for roads and above the canopy level for roofs) (Masson, 2000). Limitations are set by the maximum surface retention capacity of roofs $W_{max,rf}^{surf}$ and roads $W_{max,rd}^{surf}$, as represented by the surface water reservoirs. For natural surfaces, the various contributions from vegetation and natural subsoil are considered (Eq. 4) (Lemonsu *et al.*, 2012):

$$E_{gdn} = E_{veg} + E_{gr} + E_{gr,i} + E_s \tag{4}$$

where E_{veg} is the vegetation evapotranspiration, $E_{gr,i}$ and E_{gr} the evaporation from bare soil respectively with and without freezing, and E_s the sublimation from snow.

2.1.2 Water interception

The water content evolution in the interception water reservoirs of each surface type (denoted W_*^{surf}) is affected by precipitation and evapotranspiration rates, as indicated in Masson (2000) and Lemonsu *et al.* (2012):

$$\frac{\partial W_*^{surf}}{\partial t} = P - \frac{E_*}{L_v} \tag{5}$$

where * stands for rooftops, vegetation or bare ground surfaces.

For the road interception reservoir, the original evolution equation has been modified by including a slight water infiltration rate (I_{rd}) (m s^{-1}), since roads are never totally impervious (Ramier *et al.*, 2011):

$$\frac{\partial W_{rd}^{surf}}{\partial t} = P - \frac{E_{rd}}{L_v} - I_{rd} \tag{6}$$

I_{rd} is defined as a constant value over which the model must be calibrated.

2.1.3 Surface runoff

According to Masson (2000), when W_*^{surf} (mm) exceeds the maximum reservoir capacity ($W_{max,*}^{surf}$), surface runoff is produced (R_*^{surf}). Henceforth, it is collected by stormwater or combined sewer networks, depending on the connected effective impervious areas fraction (f_{con}) (Sutherland, 2000). Surface runoff not collected by the sewer system (($R_{rf}^{surf} + R_{rd}^{surf}) * (1 - f_{con})$) is then added to the throughfall over natural surfaces, where it can infiltrate into the subsoil with a

maximum infiltration capacity, according to the Green-Ampt approach (Abramopoulos *et al.*, 1988; Entekhabi and Eagleson, 1989; Lemonsu *et al.*, 2012).

The urban runoff R_{town} (mm s^{-1}), which is used to determine the total sewer discharge (Q_{town}^{tot}), is composed of several sources:

$$5 \quad R_{town} = R_{rf}^{surf} * f_{con} + R_{rd}^{surf} * f_{con} + R_{sew} + R_*^{subsurf} \tag{7}$$

where $R_{rf}^{surf} * f_{con}$ and $R_{rd}^{surf} * f_{con}$ are respectively the roof and the road surface runoff connected to the sewer network (mm s^{-1}); R_{sew} is the runoff in the sewer network due to soil water infiltration (mm s^{-1}), and $R_*^{subsurf}$ the subsurface runoff from each compartment (mm s^{-1}) calculated in Eq. 16.

2.1.4 Vertical water transfer

10   The surface water infiltration, as described above, constitutes an input to the subsoil of both the garden compartment and road compartment. The water is then transferred vertically (T_v) from layer to layer, accounting for the liquid water transfer and water vapour transfer stated in Boone *et al.* (2000). This process depends solely on pressure gradients, which enables taking different hydraulic soil properties into consideration. At the bottom of each soil column, the vertical water transfer is adapted by taking boundary conditions into account. The resulting outgoing water flux of the model is called deep drainage

15   D_*, which has been slightly modified for TEB-Hydro (Sect. 2.2.3).

2.2 Inclusion of hydrological processes in the urban subsoil

    In accordance with the soil description of urban gardens provided in Lemonsu *et al.* (2012), soil compartments are now considered under built-up surfaces such as roads and buildings. All three soil columns are represented by horizontal layers,

20   with an identical vertical grid in order to compute subsurface soil water transport. The thickness of each layer increases downward, with a higher grid resolution on top. In the case of the road compartment, the upper soil layers are represented by structural layers in accordance with Bouilloud *et al.* (2009). By integrating natural soil below urban surfaces, the hydrological processes in the soil (vertical water transfer and deep drainage) of both road and building compartments are being adapted from the garden compartment. Water infiltration through the road structure is thus now considered as a

25   recharge of soil moisture in the road compartment soil column. No water however is input into the building compartment soil column.

2.2.1 Horizontal water transfer

    The lateral water interactions of each soil layer among the three distinct compartments of a same grid cell have been added. In considering the structural layers of the road compartment, the horizontal transfer in the upper soil layers is computed

30   solely between the garden and building compartments. Below there, all three compartments are accounted for.

This approach is based on the principle of an exponential decay of the water content, tending towards the mean soil moisture of all three compartments, which is limited by soil moisture content at the wilting point. In assuming that the soil texture is identical in each grid cell compartment and moreover that no lateral transfer is taking place between the various grid cells of the model, the lateral intra-mesh soil moisture transfer for each soil layer is described as follows:

$$\frac{\partial W_*^{gr}}{\partial t} = -\frac{1}{\tau} * \frac{\overline{K_{sat}}}{K_i} \tag{8}$$

Updating the soil moisture content in each layer and compartment after each time step yields:

$$W_*^{gr,'} = \overline{W^{gr}} + \left(W_*^{gr} - \overline{W^{gr}}\right) * exp\left(-\left(\frac{1}{\tau} * \frac{\overline{K_{sat}}}{K_i}\right) * dt\right) \tag{9}$$

with: $\overline{W^{gr}} = \frac{\sum W_*^{gr} * f_*}{\sum f_*}$ (10)

where W_*^{gr} and $W_*^{gr,'}$ are respectively the soil moisture content for each compartment before and after horizontal balancing (m³ m⁻³), $\overline{W^{gr}}$ the mean soil moisture content of all compartments before balancing (m³ m⁻³), τ the time constant of one day, $\frac{\overline{K_{sat}}}{K_i}$ the ratio of the mean hydraulic conductivity at saturation of all three compartments to the hydraulic conductivity of each compartment, dt the numerical time step of the model(s), and f_* the fraction of each compartment.

2.2.2 Drainage of soil water by the sewer network

Various experiments and observations (Belhadj *et al.*, 1995; Lerner, 2002; Berthier *et al.*, 2004; Le Delliou *et al.*, 2009) have shown that soil water drainage occurs when artificial networks are situated under saturated soil moisture conditions. However, the ISBA soil pattern is intended to depict the unsaturated zone rather than the saturated zone. This pattern is based on a representation of the soil moisture state in agronomic terms (i.e. water content at wilting point, field capacity and saturation). When taking this into account, the infiltration rate into the sewer network (I_{sew} in m s⁻¹) is described in such a way that the hydraulic conductivity of the network soil layer ($k_{sew}(W_{gr})$ (m s⁻¹)) is its limiting factor, with a maximum value at saturation of:

$$I_{sew} = k_{sew}(W_{gr}) * I_p * D_{sew} \tag{11}$$

where I_p is a calibration parameter, without any physical significance, representing the water tightness of the sewer pipe (-), and D_{sew} the sewer density within a single grid cell (-) expressed by the ratio of the total sewer length in one grid cell (m) to the maximum total sewer length in a single grid cell of the entire study site (m). Let's note that this formulation has been adapted to TEB-Hydro from Rodriguez *et al.* (2008).

2.2.3 Deep drainage

In cities, artificial networks may play the role of rivers and thus contribute to draining soil water by means of infiltration. It has therefore been envisaged to limit deep drainage in order to favour soil water infiltration into the sewer networks during

wet periods. For this purpose, the soil moisture emerging from the last layer of the model is partially or totally retained, according to a coefficient C_{rech}, until complete layer saturation. At each time step, the soil moisture content in the last layer n is thus updated according to:

$$W_*^{gr,n} = W_*^{gr,n} + W_*^{gr,flux,n} * C_{rech} \qquad (12)$$

And the deep drainage becomes: $D_* = W_*^{gr,flux,n} * (1 - C_{rech}) * d_n * \rho/dt \qquad (13)$

where $W_*^{gr,n}$ is the soil moisture content of the last layer n (m³ m⁻³), $W_*^{gr,flux,n}$ the soil moisture content derived from the outgoing water flux (m³ m⁻³), C_{rech} the coefficient of retention (-), D_* the deep drainage (mm s⁻¹), d_n the thickness of the last layer, ρ the water density (kg m⁻³), and dt the numerical time step of the model(s).

If the deep layer is saturated, the excess moisture rises from layer to layer, with:

The soil moisture content in upper layer i-1: $W_*^{gr,i-1,'} = W_*^{gr,i-1} + \max\left(0, W_*^{gr,i} - W_{*,sat}^{gr,i}\right) * \frac{d_{i-1}}{d_i} \qquad (14)$

The soil moisture content remaining in layer i: $W_*^{gr,i,'} = \min(W_*^{gr,i}, W_{*,sat}^{gr,i}) \qquad (15)$

If saturation reaches the surface layer, then the excess moisture is added to subsurface runoff:

$$R_*^{subsurf,'} = R_*^{subsurf} + \max\left(0, W_*^{gr,1} - W_{*,sat}^{gr,1}\right) * \frac{d_1}{dt} * \rho \qquad (16)$$

where $W_{*,sat}^{gr,i}$ is the soil moisture content at saturation (m³ m⁻³), $W_*^{gr,i,'}$ and $W_*^{gr,i}$ respectively the soil moisture content in current layer i, after and before update (m³ m⁻³), $W_*^{gr,i-1,'}$ and $W_*^{gr,i-1}$ respectively the soil moisture content in upper soil layer i-1, after and before update (m³ m⁻³), $\frac{d_{i-1}}{d_i}$ (-) the ratio of layer thicknesses between upper layer i-1 and lower layer i, and $R_*^{subsurf,'}$ and $R_*^{subsurf}$ respectively the subsurface runoff after and before update (mm s⁻¹).

2.3 TEB-Hydro output variables

In addition to the simulated hydrological output variables calculated in TEB-Veg (latent heat fluxes on all surfaces, soil moisture in each soil layer ($W_{gdn}^{gr,i}$) and deep drainage (D_{gdn}) of the garden compartment), the TEB-Hydro model simulates the soil moisture in each soil layer ($W_*^{gr,i}$) and the deep drainage (D_*) under artificial surfaces. Other new model output variables include urban runoff (R_{town}), with its components stemming from rooftops ($R_{rf}^{surf} * f_{con}$) and road surfaces ($R_{rd}^{surf} * f_{con}$), soil water infiltration into the sewer network (R_{sew}), and the subsurface runoff from each compartment ($R_*^{subsurf}$).

3. Experimental study areas and observation data

The experimental data are derived from two small urban catchments in the city of Nantes (France). The properties of these catchments, along with local observation data and the meteorological forcing data of the model will be described below.

3.1 Experimental data

5 #### 3.1.1 Rezé catchment

The Rezé experimental site is located in the southern part of the city of Nantes, close to the Atlantic coast (Fig. 2). It was instrumented (with measurements of precipitation, discharge from the rainwater network and soil water) from 1993 to 1998, and a complete continuous database is available for that period. The climate is oceanic with an average annual rainfall of approx. 830 mm during this period; the year 1994 was the wettest one.

10 The 4.7-ha basin is entirely residential, comprising single-family homes with private gardens. The separate sewer network is divided into wastewater and stormwater with lengths of 803 m and 480 m, respectively. The impervious surface of the catchment accounts for 45% of the total area, of which 84% is connected to the stormwater system. A detailed site description can be found in Berthier *et al.* (1999) and Dupont *et al.* (2006) (Tab. 1).

The Rezé catchment and its database have been the subject of several studies (Rodriguez *et al.*, 2003; Berthier *et al.*, 2004;
15 Dupont *et al.* (2006); Lemonsu *et al.*, 2007; Rodriguez *et al.*, 2008). Berthier (1999) modelled the role of soil in generating urban runoff on the Rezé catchment. He studied both the hydrological aspects and site observations. Among other emphases, he examined the discharge observed in the wastewater sewer during the winter periods between 1993 and 1997 before estimating the discharge due to soil water infiltration and compared this value with the simulated base flow in the sewer network.

20 #### 3.1.2 Pin Sec catchment

The Pin Sec experimental site is located in the eastern section of Nantes; it has been a part of the Nantes Observatory for the Urban Environment (ONEVU) since 2006 and thus contains a dense network of continuous measurement equipment (rain gauges, flow meters in networks, piezometers, tensiometers and micro-climatological masts). In correspondence with the simulation period of this study, rainfall patterns were analysed between May 2010 and September 2012, with an annual
25 rainfall of approx. 700 mm for the year 2011.

The catchment area spans 31 ha with some 2,500 inhabitants (Le Delliou *et al.*, 2009). The northern part of the site is characterised by single-family housing with private gardens, unlike the southern part, which encompasses 4-storey multi-family buildings with public parks (Fig. 2b). The sewer network is separate, divided into wastewater and stormwater with respective lengths of 6,973 m and 3,911 m. 51% of the total area is impervious, of which only 61% has been found (survey
30 conducted by the Nantes Metropolitan government) to be connected to the stormwater sewer. A description of this catchment is summarised in Tab. 1.

3.2 Meteorological forcing

Forcing the model with observations requires atmospheric data, such as precipitation, temperature, specific humidity, atmospheric pressure, wind speed and direction, and incoming shortwave and longwave radiation. For both experimental sites, the precipitation rates (no snowfall for all simulation periods) were collected on site by means of rain gauges.

5   All other forcing data were generated from the data of the nearby Météo-France weather station (at Nantes Airport), including incoming solar radiation, cloudiness, pressure, air temperature and humidity at 2 m above ground, and wind speed at 10 m above ground. To avoid the direct influence of the urban canopy, the forcing level height for temperature, humidity and wind had to be set above the roughness sublayer top, hence the atmospheric data had to be adjusted accordingly (Lemonsu *et al.*, 2012).

10   ### 4. Evaluation of the TEB-Hydro model

The TEB-Hydro model was evaluated by comparing the simulated with the observed total sewer discharge and the portion of this discharge due to soil water infiltration. Observations were derived from the two experimental sites described above. Let's note that the local properties of these sites, as well as the simulation period, do vary. A sensitivity analysis performed on the Rezé catchment will be presented first. The hydrological parameters taken into account consist of: the maximum

15   retention capacity of the artificial surfaces $W_{max,*}^{surf}$ (roads and buildings), a parameter describing the water-tightness of the sewer pipe I_p, the maximum infiltration rate through the road structure I_{rd}, the fraction of impervious surface areas connected to the sewer network f_{con}, and the deep drainage D_* (Sect. 2 and Tab. 2). In addition, possible combined effects of these studied parameters will also be analysed. As is typical with hydrological models, the model is calibrated on those parameters where it shows the greatest sensitivity. Next, the model will be evaluated on the observed total sewer discharge

20   of both the Rezé and Pin Sec catchments. Simulations will be run with the TEB-Hydro model and then compared to observations in order to discuss the performance of recent model developments.

4.1 Model configuration

The TEB-Hydro model (SURFEX v7.3) has been applied to a single grid point (1D) for both experimental sites; it operates in "off-line" mode, forced by meteorological observations (Sect. 3.2), with a one-hour time step. The model's numerical time

25   step is 5 min. For both catchments, 12 soil layers were taken into account, and the road structure was divided into 5 artificial layers. By virtue of the mean sewer system depth (1.50 m), the sewer pipe is thus situated in the 10th soil layer. Natural surfaces are represented by bare ground, low and high-growth vegetation.

In the case of the Rezé catchment, the model was run over a 6-year period, from January 1993 to December 1998. The hydrological year starts in September, as the lowest base flow can be detected in August for the Nantes region. Its

30   morphological data, radiative and thermal properties of the materials (TEB), and soil and vegetation properties (ISBA) have all been considered, like in Lemonsu *et al.* (2007).

The simulation period for the Pin Sec catchment is 2.5 years, i.e. between May 2010 and September 2012. The morphological site data, radiative and thermal properties of the materials (TEB), and soil and vegetation properties (ISBA) were determined on the basis of several sources (FluxSAP database (Furusho, 2012), Nantes Metropolitan urban databank, and Ecoclimap I (Faroux *et al.*, 2013)). Due to inconsistencies between previous studies (Le Delliou *et al.*, 2009; Seveno *et al.*, 2014), the Pin Sec catchment area has been re-delimited using a GIS (Fig. 2b).

4.2 Sensitivity analysis

The sensitivity analysis was solely conducted on the Rezé catchment; its aim was to better understand the role of each individual parameter on the various hydrological processes and identify those responsible for greater model sensitivity and thus requiring calibration. In general, two types of analyses were conducted: local and global (Saltelli *et al.*, 2004; Tang *et al.*, 2006). For this study, a local analysis based on the One Factor at a Time (OFAT) method was chosen (Montgomery, 2017). This approach measures the influence of a parameter by the amplitude in variation of the model's response around a nominal value of this parameter. The sensitivity analysis encompasses several hydrological parameters, with a range of realistic values (minimum, nominal, maximum). These values have been identified from either a literature review or *in situ* measurements (Berthier *et al.*, 1999; Lemonsu *et al.*, 2007; Furusho *et al.*, 2013) (Tab. 2). The REF simulation is based on the nominal values of all parameters. The MIN and MAX simulations can consistently be performed when a single parameter is changed respectively to its minimum and maximum values, while the other parameters remain fixed at their nominal values.

Moreover, a two-level factorial plan of 2^3 is presented in order to determine whether or not some parameters (I_p, I_{rd} and D_*) display combined effects on the model output and then dissemble the interactions taking place between them. Such a design is of common use in experiments involving several interlinked factors (Montgomery, 2007).

Each parameter is assigned two levels, which serves to limit the experimental domain. In the current case, the domain of each parameter corresponds to the margins set for the sensitivity analysis. The higher level will hereafter be denoted +1 for the MAX parameter value and -1 for the lower value corresponding to the parameter MIN value (Tab. 3). To take all possible parameter combinations into account, a matrix is generated with all values being arranged according to the "Yates Order". The principal effects (Eq. 17) of the given parameters and the effects of their interactions (Eq. 18) are then calculated, in direct correlation with the mean response of both its low level ($\bar{y}_{*-}$) and high level ($\bar{y}_{*+}$). The dependence of two parameters can be analysed visually by showing the effects of both parameters on the model response ($\bar{y}_*$): two perfect parallel lines would not indicate any interdependence between the two factors, as opposed to non-parallelism.

In the current context, $\bar{y}_*$ corresponds to the maximum observed sewer discharge due to soil water infiltration $Q_{sew,max}$ during winter 1994/95 in the Rezé catchment. A positive effect stands for an increase of this process while transitioning from the low parameter level (-1) (MIN value) to its high value (+1) (MAX value), and *vice versa* in the case of a negative effect:

$$e(A) = \bar{y}_{A+} - \bar{y}_{A-} \tag{17}$$

$$e(AB) = \bar{y}_{AB+} - \bar{y}_{AB-} \tag{18}$$

where $e(A)$ is the principal effect of a parameter called A, $e(AB)$ the effect of the interaction between two different parameters A and B, $\bar{y}_{*+}$ the mean response of all combinations where the parameter or the interaction of two parameters is at its high level (+1), and $\bar{y}_{*-}$ the mean response of all combinations where the parameter or the interaction of two parameters is at its low level (-1).

4.3 Comparative method

In the case of the sensitivity analysis, the Kling-Gupta statistical criterion (KGE) has been calculated from the output variables of the MIN or MAX simulations as $D_{sim}(t)$, and from the output variables of the REF simulation as $D_{ref}(t)$ (Eqs. 19 to 22). For the model calibration and evaluation phase, $D_{ref}(t)$ is replaced by observed data $D_{obsf}(t)$. The Kling-Gupta efficiency (KGE) coefficient is a synthesis of several criteria varying between 1 and -∞ (Gupta *et al.*, 2009):

$$KGE = 1 - \sqrt{(r-1)^2 + (\alpha - 1)^2 + (\beta - 1)^2} \tag{19}$$

With the linear correlation coefficient (r):

$$r = \frac{\sum((Dsim(t) - \overline{Dsim}) * (Dref(t) - \overline{Dref}))}{\sqrt{\sum(Dsim(t) - \overline{Dsim})^2} * \sqrt{\sum(Dref(t) - \overline{Dref})^2}} \tag{20}$$

With the relative variability (α) represented by the standard deviation:

$$\alpha = \frac{\sqrt{\sum(Dsim(t) - \overline{Dsim})^2}}{\sqrt{\sum(Dref(t) - \overline{Dref})^2}} \tag{21}$$

And the bias (β):

$$\beta = \frac{\overline{Dsim}}{\overline{Dref}} \tag{22}$$

The results of the Kling-Gupta efficiency (KGE) criteria are then presented for each MIN and MAX simulation. For this analysis, the chosen model output variables depend on the influence of the parameter on the hydrological processes, namely:

- Urban runoff (R_{town}) and the subsequent total urban discharge (wastewater and stormwater sewer) (Q_{town}^{tot});
- Soil water drainage via the sewer network (R_{sew}).

4.4 Calibration

Based on the outcomes of the sensitivity analysis, the model is then calibrated. The first few months of the spin-up simulation period are systematically excluded in order to anticipate problems upon initialising the model's prognostic variables. Calibration is applied transversally, meaning that after removing the spin-up time from the simulation period, it is split into two equal periods, and the model is calibrated and evaluated on both of them. By doing so, the model will first be calibrated on the first period and then evaluated on the second in following the same process by inversing calibration and

evaluation periods. The simulations are then compared with the observed total sewer discharge and, like for the sensitivity analysis (Sect. 4.3), the KGE criterion is calculated along with its components.

5. Results and discussion

5.1 Sensitivity analysis

5 As shown in Tab. 4, the KGE coefficients for both the MIN and MAX simulations specific to maximum retention capacity of the surface reservoir of roads ($W^{surf}_{max,rd}$) and roofs ($W^{surf}_{max,rf}$) show little difference for both the urban runoff and runoff due to soil water infiltration (Figs. 3a and 3b). In the case of maximum roof retention capacity, urban runoff is mainly influenced by small rainfall events.

In terms of urban runoff, the model does not show any higher sensitivity to the parameter describing the infiltration rate

10 through the road (I_{rd}) than to $W^{surf}_{max,rd}$ and $W^{surf}_{max,rf}$ (Tab. 4). Such is not the case however when considering the sewer runoff due to soil water infiltration. As the road infiltration rate increases, total surface runoff decreases but only for small rain events (Fig. 4a). Also, soil moisture rises within the soil layers, thus boosting soil water infiltration into the sewer network (Fig. 4b).

As expected, the model is more sensitive to the fraction of impervious surfaces connected to the sewer system (f_{con}) (Fig. 5).

15 The bias (β) and relative variability (α) (Tab. 4) reveal different values for MIN and MAX simulations, yet they both lead to the same KGE criterion (Tab. 4). The variation in the f_{con} parameter influences urban runoff as well as sewer runoff due to soil water infiltration. A low connection rate leads to a lower urban runoff, while a greater parameter value increases urban runoff (Fig. 5). The runoff from surfaces not connected to the sewer system feeds the infiltration towards the natural surfaces. The amount of infiltrated water in the garden compartment thus changes with this parameter, thereby influencing

20 the soil moisture in all layers and compartments. These values are higher when the fraction of connected surfaces is low and, conversely, lower with a high fraction.

The calculated KGE values (Tab. 4) are quite divergent between the MIN and MAX simulations for parameters I_p and D_* with both output variables, which implies that the model is very sensitive to them. In addition, the results of the factorial plan (Fig. 6), based on the calculated direct effects on the maximum sewer discharge due to soil water infiltration, corroborate

25 these results.

As for the parameter describing the water-tightness of the sewer pipe (I_p), its increase leads to higher peaks of infiltration into the sewer network (Fig. 7a) but does not influence the infiltration period. Moreover, the calculated effect of an I_p of +2.9E-04 signifies an increase in soil water infiltration into the sewer network when transitioning from its low level (-1) to its high one (+1) (Fig. 6). In fact, soil water drainage via the sewer network is as important as a degraded network condition

30 (cracks, root penetration, etc.), and soil moisture at the network location is close to saturation.

As for the deep drainage parameter (D_*), the negative effect (Fig. 6) indicates that infiltration declines with an increasing parameter value. As seen in Fig. 7b, limiting deep drainage to a magnitude of 10% (MAX) does not generate a significant difference with the reference simulation in assessing sewer discharge due to soil water infiltration. Blocking the deep drainage completely (MIN) however leads to a saturation of the lower soil layers, thus adding to the soil water infiltration into the sewer network (Fig. 7b).

As was the case for water-tightness of the sewer pipe (I_p), both the infiltration rate through the road (I_{rd}) and deep drainage (D_*) seem to influence the sewer drainage due to soil water infiltration, with the effects of their interactions having been calculated and visualised. In this manner, the I_p/D_* interaction can be highlighted as the most influential of all three first-order interactions (Fig. 6). In addition, Figure 8 effectively shows the correlation between the two parameters (see the two lines run non-parallel to one another), whereas the correlations between the other parameters appear to be less significant.

In comparing model sensitivity among the 6 parameters for both urban runoff and runoff due to soil water infiltration, it can be concluded that the model is less sensitive to changes in parameters $W_{max,rd}^{surf}$ and $W_{max,rf}^{surf}$. Four parameters can thus be singled out for calibration:

- The parameter describing the water-tightness of the sewer pipe (I_p)
- Infiltration rate through the road (I_{rd})
- The fraction of impervious surfaces connected to the sewer network (f_{con})
- Deep drainage (D_*).

5.2 Model calibration and evaluation

In considering the results of the sensitivity analysis, this model needs to be calibrated on four parameters. Yet for both catchment areas, the parameter f_{con} has been determined during exhaustive field surveys and therefore is well known. Consequently, this parameter will be neglected, hence only the three remaining parameters are considered for calibration. Four different values within the predefined range of the sensitivity analysis are tested for each parameter (Tab. 5). The model is calibrated and evaluated on the total observed sewer discharge (Q_{town}^{tot}), as determined from the model outcome variable: urban runoff (R_{town}). However, since the drainage capacity of soil water through the sewer network can be extensive in urban areas, the share of sewer discharge originating from soil water infiltration (Q_{sew}) has been investigated in detail. Hence, the choice of this parameter's values also depends on the findings of the sensitivity analysis with respect to this output variable (Q_{sew}). In Section 5.1, it was shown that soil water infiltration into the sewer increases as the I_p value rises, as opposed to parameters I_{rd} and D_*. The range of values has thus been set close to the maximum I_p value and minimum I_{rd} and D_* values. Totally blocking the deep drainage however is not an option, since in reality soil water is not only drained by artificial sewer systems but moreover can find other pathways within the urban subsoil (groundwater recharge, seepage, etc.).

5.2.1 Rezé catchment

In the Rezé catchment, the calibration and evaluation periods have been compounded by two consecutive hydrological years, i.e. from September 1993 to August 1995, and from September 1995 to August 1997.

The KGE criterion results indicate a clear and constant trend for all simulations, independently of the considered time period

5   (Fig. 9) or the value of parameter D_*:

For starters, as seen in the example (deep drainage limited to 2%), all KGE criteria are far better for the first period from 1993 to 1995 than for the second (1995-97) (Fig. 9). This discrepancy between the two simulation periods is primarily related to the KGE criterion component bias (β), which shows a greater bias for the second simulation period (Fig. 9).

Secondly, the smallest value of I_p achieves a better result than the highest value, when assessing total sewer discharge.

10   Thirdly, the parameter I_{rd} does not exert significant influence on the simulated total sewer discharge, since the criterion does not vary much among its different values.

The correlation (r) of simulated and observed discharge peaks is satisfactory, with values of about 0.90 for both simulation periods and all simulation configurations (Fig. 9). The model displays a tendency to overestimate the observed total sewer discharge (Fig. 10), more so for the second simulation period, showing greater variability (α) through all simulations (Fig. 9).

15   Regardless of the deep drainage values, simulation 13 seems to stand out with a KGE between 0.79 and 0.82 over the entire simulation period. The KGE values range between 0.81 and 0.84 for the first period and between 0.66 and 0.68 for the second. In examining both simulation periods separately, simulation 14 seems to perform slightly better for the first period. Given the fact that simulation 13 performs much better over the second period than simulation 14, simulation 13 should also be tagged for a transversal calibration. The degradation in KGE during the second year is mainly related to the higher bias

20   values, most likely caused by the various hydrological properties of both simulation periods. For the first period 1993-95, a total precipitation height of approx. 1,873 mm with a very wet winter during 1994-95 can be observed, whereas the second period is much dryer posting just 1,302 mm.

As regards total sewer discharge, the best combination of parameters would be to set parameter I_p at 0.09 and I_{rd} at 10^{-5}, whereas parameter D_* can vary. We will thus be examining in greater detail the portion of sewer discharge due to soil water

25   infiltration, with parameter D_* influencing this process significantly. Berthier (1999) observed a maximum sewer discharge due to soil water infiltration of about 0.008 m^3 h^{-1} lm^{-1} during the winter 1994-95. Accounting for the total sewer length of 1,283 m at the Rezé catchment would yield a maximum sewer infiltration rate of roughly 10.3 m^3 h^{-1}. Limiting deep drainage to 2% produces (Fig. 11a) a simulated discharge peak of 4.8 m^3 h^{-1} during this period, which is much less than observation findings. In looking at the simulation with a limited deep drainage (D_*) of 1%, the observed discharge peak becomes

30   significantly overestimated at 27 m^3 h^{-1} (Fig. 11b). In the aim of evaluating the model as well on the sewer discharge due to soil water infiltration, deep drainage should be limited somewhere between 1% and 2%.

Another option would consist of focusing on the I_p parameter since the sensitivity analysis also revealed its influence on the process of soil water infiltration into the sewer. As stated above, raising the value of I_p is beneficial for the infiltration rate.

Hence, simulation 14 would be more suitable, as I_p has been set at 0.3 while I_{rd} remains at 10^{-5}. In conjunction with deep drainage limited to 2%, the maximum sewer discharge due to soil water infiltration during winter 1994-95 equals roughly 10.6 m³ h⁻¹, which is close to the observed discharge (Fig. 11c). For this combination of parameters (i.e. I_p =0.3, I_{rd}=10^{-5}, D_*=2), the KGE criterion based on total sewer discharge is slightly better, like for simulation 13, with a value of 0.86 for the

5   first period. Such is not the case however for the second period, with a value of 0.57.

5.2.2 Pin Sec catchment

For the Pin Sec catchment, the period between September 2010 and August 2011 has been compared to the period from September 2011 to August 2012 and *vice versa*.

As was the case with the Rezé catchment, the same trends and tendencies can be observed independently of the simulation

10   periods and configurations. Simulation 13 can once again be cited as the best configuration of parameters, with a KGE criterion of 0.79 over the whole simulation period. Parameter I_p can thus be set at 0.09 and I_{rd} at 10^{-5}, whereas D_* is variable.

5.2.3 General discussion

In terms of calibration and evaluation processes, this model exhibits the tendency to overestimate the observed total sewer discharge. This skewing can be explained by the choice of setting parameter f_{con} at its real value rather than calibrating the

15   model on it. This parameter is indeed the one exerting a predominant influence on total sewer discharge, since it directly conditions the surface runoff of impervious surfaces. When calibrating the model on total sewer discharge, it is thus essential to take this parameter into account in case it is not well known, as opposed to other parameters I_{rd} and D_* that exercise little influence over this process. Evaluating the model from the standpoint of sewer discharge due to soil water infiltration however requires a more detailed consideration of I_p and D_*. The water exchanges taking place between the urban subsoil

20   and both the natural and sewer network are critical processes in urban areas. As shown above, the model is very sensitive to them and comparing them to observation findings can help improve the simulated urban water budget, yet experimental data on such fluxes are indeed rare.

For both catchments, the statistical criteria indicate the same trend throughout all simulation configurations and periods, with a better KGE for the first period. The model seems to perform better under wetter climatic conditions. The best simulation

25   configuration is the same irrespective of calibrating the model on the first or second period, with the exception of Simulation 14. It thus proves necessary to apply the model more extensively in regions with different meteorological patterns in order to investigate whether the model could operate under different meteorological conditions (dry and wet periods), which is an essential condition for projection applications. The same simulation configuration yields the best results for both the Rezé and Pin Sec catchments. Considering their differences in terms of soil texture and urban patterns (mean building height), this

30   is an encouraging result for working at the city scale, as spatial heterogeneity no longer constitutes an obstacle.

6. Conclusion

The objective of this study has been to contribute to developing a complete urban hydro-microclimate model and testing the ability of this model to replicate hydrological processes. This goal has been achieved given that the representation of hydrological processes in the TEB-Veg model (Lemonsu *et al.*, 2012) has been extended and refined. The new model

5 version, called TEB-Hydro, has been developed by taking a detailed representation of the urban subsoil into account. This step has enabled horizontal interactions of soil moisture between the urban subsoil of built-up and natural surfaces within a single grid-cell. Furthermore, the drainage of soil water via the sewer network has been introduced in the road compartment of the model. Deep drainage, which normally supplies the base flow of the natural river network, has been limited to favouring humidification of the lower soil layers, resulting in more realistic infiltration patterns into the sewer network under

10 urban conditions. A sensitivity analysis has been performed in the aim of better understanding the influences of model parameters on these processes and identifying the parameters to serve calibration purposes. Six parameters were investigated, of which four seemed to significantly influence the model output in terms of total sewer discharge and the portion of discharge caused by soil water infiltration, namely: the parameter (I_p) describing the water-tightness of the sewer pipe, the road infiltration rate (I_{rd}), the fraction of impervious surfaces connected to the sewer network (f_{con}), and the

15 parameter (D_*) that enables limiting deep drainage out of the urban subsoil.

TEB-Hydro was then applied to two small residential catchments located close to the city of Nantes (France). In both cases, the model was calibrated and evaluated on the observed sewer discharge, in displaying the same hydrological behaviour. The total sewer discharge is consistently being overestimated, independent of both simulation period and configuration. Considering parameter f_{con} as a calibration element, should it not be known, allows tackling this problem. The model seems

20 to function better under wet conditions, since simulation period 1 offers better KGE results. In assessing the entire simulation periods for both catchments, the same parameter configuration stands out, independently of meteorological and local physical conditions, thus implying that the model is running in a coherent and steady manner. This finding would need to be confirmed by applying the model to several catchments areas outside of Nantes. In conclusion, the evaluation outcomes laid out herein are encouraging for application of the model at the city scale for purposes of projecting global change.

25 Lastly, a more detailed representation of the urban subsoil and its hydrological pattern enhances the model's urban water budget. Given that the water and energy budgets are coupled, it is likely that the energy budget of the model is improved at the same time. An upcoming research project is underway, which entails investigating alongside the hydrological processes energy patterns like latent and sensible heat fluxes.

7. Code and data availability

30 The surface modelling platform SURFEX is accessible on open source, where the codes of surface schemes TEB and ISBA can be downloaded (http://www.cnrm-game-meteo.fr/surfex/). This platform is regularly updated; however, the model

5   Rezé and Pin Sec catchment databases are available upon request submitted to the authors of the Water and Environment Laboratory of the French Institute of Science and Technology for Transport, Development and Networks (IFSTTAR).

References

Abramopoulos, F.; Rosenzweig, C. and Choudhury, B.: Improved Ground Hydrology Calculations for Global Climate Models (GCMs): Soil Water Movement and Evapotranspiration, *Journal of Climate, 1*, 921-941, 1988.

10   Bach, P. M., Rauch, W., Mikkelsen, P. S., Mc Carthy, D. T., and Deletic, A.: A critical review of integrated urban water modelling – Urban drainage and beyond . *Environmental Modelling & Software , 54*, 88-107, 2014.

Belhadj, N.; Joannis, C. and Raimbault, G.: Modelling of rainfall induced infiltration into separate sewerage. *Water Science and Technology , 32*, 161 - 168, 1995.

Berthier, E.: Contribution à une modélisation hydrologique à base physique en milieu urbain: Elaboration du modèle et

15   première évaluation, Université Joseph-Fourier (UJF), Institut National Polytechnique de Grenoble, Grenoble, 1999.

Berthier, E., Andrieu, H., and Rodriguez, F.: The Rezé urban catchments database. *Water Resources Research, 35*(6), 1915-1919, 1999.

Berthier, E., Andrieu, H., and Creutin, J.: The role of soil in the generation of urban runoff: development and evaluation of a 2D model . *Journal of Hydrology , 299*(3–4), 252-266, 2004.

20   Berthier, E., Dupont, S., Mestayer, P. and Andrieu, H.: Comparison of two evapotranspiration schemes on a sub-urban site *Journal of Hydrology , 328*, 635 - 646, 2006.

Betts, R. A.: Implications of land ecosystem-atmosphere interactions for strategies for climate change adaptation and mitigation, Tellus B. *Chemical and Physical Meteorolgy, 59:3,* 602-615, 2007.

Boone, A., Masson, V., Meyers, T., and Noilhan, J.: The Influence of the Inclusion of Soil Freezing on Simulations by a

25   Soil–Vegetation–Atmosphere Transfer Scheme. *Journal of Applied Meteorology, 39*, 1544–1569, 2000.

Bouilloud, L., Martin, E., Habets, F., Boone, A., Moigne, P. L., Livet, J., Marchetti, M., Foidart, A., Franchistéguy, L., Morel, S., Noilhan, J. and Pettré, P. Road Surface Condition Forecasting in France. *Journal of Applied Meteorology and Climatology*, *48*, 2513-2527, 2009.

DHI: Mike Urban cs: Building a simple Mouse Model in Mike Urban. Step-by-step Training Guide, 2001.

30   Dupont, S.: Modélisation dynamique et thermodynamique de la canopée urbaine: réalisation du modèle de sols urbains pour SUBMESO, Ecole Doctorale Méchanique Thermique et Génie Civil, Université de Nantes, Nantes, 2001.

Dupont, S., Mestayer, P. G., Guilloteau, E., Berthier, E. and Andrieu, H.: Parameterization of the Urban Water Budget with the Submesoscale Soil Model. *Journal of Applied Meteorology and Climatology, 45,* 624-648, 2006.

EC (European Commission): Towards an EU Research and innovation agenda for nature-based solutions and re-naturing cities, Brussels: CEC, 2015.

EEA: *Urban adaptation to climate change in Europe: Challenges and opportunities for cities together with supportive national and European policies.* Tech. rep., European Environment Agency, EEA Copenhagen, 2012.

Entekhabi, D. and Eagleson, P. S.: Land Surface Hydrology Parameterization for Atmospheric General Circulation models Including Subgrid Scale Spatial Variability. *Journal of Climate, 2,* 816-831, 1989.

Faroux, S.; Kaptué Tchuenté, A. T.; Roujean, J.-L.; Masson, V.; Martin, E. and Le Moigne, P.: ECOCLIMAP-II/Europe: a twofold database of ecosystems and surface parameters at 1 km resolution based on satellite information for use in land surface, meteorological and climate models. *Geoscientific Model Development, 6*, 563-582, 2013.

Fletcher, T., Andrieu, H., and Hamel, P.: Understanding, management and modelling of urban hydrology and its consequences for receiving waters: A state of the art . *Advances in Water Resources , 51*, 261-279, 2013.

Furusho, C: Base de données FluxSAP IRSTV - Projet ANR-VegDUD, 2012.

Grimmond, C. S. B.; Blackett, M.; Best, M. J.; Baik, J.-J.; Belcher, S. E.; Beringer, J.; Bohnenstengel, S. I.; Calmet, I.; Chen, F.; Coutts, A.; Dandou, A.; Fortuniak, K.; Gouvea, M. L.; Hamdi, R.; Hendry, M.; Kanda, M.; Kawai, T.; Kawamoto, Y.; Kondo, H.; Krayenhoff, E. S.; Lee, S.-H.; Loridan, T.; Martilli, A.; Masson, V.; Miao, S.; Oleson, K.; Ooka, R.; Pigeon, G.; Porson, A.; Ryu, Y.-H.; Salamanca, F.; Steeneveld, G.; Tombrou, M.; Voogt, J. A.; Young, D. T. and Zhang, N.: Initial results from Phase 2 of the international urban energy balance model comparison. *International Journal of Climatology, John Wiley & Sons, Ltd., 31*, 244-272, 2011.

Gros, A.; Bozonnet, E.; Inard, C. and Musy, M.: Simulation tools to assess microclimate and building energy – A case study on the design of a new district. *Energy and Buildings, 114*, 112 - 122, 2016.

Gupta, H. V.; Kling, H.; Yilmaz, K. K. and Martinez, G. F.: Decomposition of the mean squared error and NSE performance criteria: Implications for improving hydrological modelling. *Journal of Hydrology, 377*, 80-91, 2009.

Hamel, P., Daly, E., and Fletcher, T. D.: Source-control stormwater management for mitigating the impacts of urbanisation on baseflow: A review . *Journal of Hydrology , 485*, 201-211, 2013.

Le Delliou, A.-L., Rodriguez, F. and Andrieu, H.: Modélisation intégrée des flux d'eau dans la ville - impacts des réseaux d'assainissement sur les écoulements souterrains. *La Houille Blanche,* 152-158, 2009.

Lemonsu, A., Masson, V., and Berthier, E.: Improvement of the hydrological component of an urban soil–vegetation–atmosphere–transfer model. *Hydrological Processes, 21*(16), 2100-2111, 2007.

Lemonsu, A., Masson, V., Shashua-Bar, L., Erell, E., and Pearlmutter, D.: Inclusion of vegetation in the Town Energy Balance Model for modeling urban green areas. *Geoscientific Model Development, 5*, 1377-1393, 2012.

Lerner, D. N.: Identifying and quantifying urban recharge: a review. *Hydrogeology Journal, 10*, 143-152, 2002.

Malys, L.; Musy, M. and Inard, C.: Direct and Indirect Impacts of Vegetation on Building Comfort: A Comparative Study of Lawns, Green Walls and Green Roofs. *Energies, 9*, 2016.

Mitchell, V. G.; Cleugh, H. A.; Grimmond, C. S. B. and Xu, J.: Linking urban water balance and energy balance models to analyse urban design options. *Hydrological Processes, John Wiley & Sons, Ltd., 22*, 2891-2900, 2008.

5   Masson, V.: A Physically-Based Scheme For The Urban Energy Budget In Atmospheric Models. *Boundary-Layer Meteorology, 94*(3), 357-397, 2000.

Masson, V.; Le Moigne, P.; Martin, E.; Faroux, S.; Alias, A.; Alkama, R.; Belamari, S.; Barbu, A.; Boone, A.; Bouyssel, F.; Brousseau, P.; Brun, E.; Calvet, J.-C.; Carrer, D.; Decharme, B.; Delire, C.; Donier, S.; Essaouini, K.; Gibelin, A.-L.; Giordani, H.; Habets, F.; Jidane, M.; Kerdraon, G.; Kourzeneva, E.; Lafaysse, M.; Lafont, S.; Lebeaupin Brossier, C.;

10 Lemonsu, A.; Mahfouf, J.-F.; Marguinaud, P.; Mokhtari, M.; Morin, S.; Pigeon, G.; Salgado, R.; Seity, Y.; Taillefer, F.; Tanguy, G.; Tulet, P.; Vincendon, B.; Vionnet, V. and Voldoire, A.: The SURFEXv7.2 land and ocean surface platform for coupled or offline simulation of earth surface variables and fluxes. *Geoscientific Model Development, 6,* 929-960, 2013.

Montgomery, D. C.: University, A. S. (Ed.) Design and Analysis of Experiments, John Wiley &Sons Inc., 2017.

Musy, M.; Malys, L.; Morille, B. and Inard, C.: The use of SOLENE-microclimat model to assess adaptation strategies at the

15 district scale. *Urban Climate, 14*, 213 - 223, 2015.

Oke, T.: *Boundary Layer Climates* (éd. 2d ed). (Routledge, Éd.), 1987.

Ramier, D.; Berthier, E. and Andrieu, H.: The hydrological behaviour of urban streets: long-term observations and modelling of runoff losses and rainfall–runoff transformation. *Hydrological Processes, John Wiley & Sons, Ltd., 25*, 2161-2178, 2011.

Rodriguez, F.; Andrieu, H. and Creutin, J.-D.: Surface runoff in urban catchments: morphological identification of unit

20 hydrographs from urban databanks. *Journal of Hydrology , 283*, 146 - 168, 2003.

Rodriguez, F., Andrieu, H., and Morena, F.: A distributed hydrological model for urbanized areas – Model development and application to case studies . *Journal of Hydrology , 351*(3–4), 268-287, 2008.

Rossman, L. A.: Storm water management model user's manual, version 5.0 National Risk Management Research Laboratory, Office of Research and Development, US Environmental Protection Agency Cincinnati, 2010.

25 Salvadore, E., Bronders, J., and Batelaan, O.: Hydrological modelling of urbanized catchments: A review and future directions . *Journal of Hydrology , 529, Part 1*, 62-81, 2015.

Saltelli, A.; Tarantola, S.; Campolongo, F. and Ratto, M.: Sensitivity Analyseis in Practice: a guide to assessing scientific models, John Wiley & Sons, Ltd, 2004.

Schirmer, M., Leschik, S., and Musolff, A.: Current research in urban hydrogeology – A review . *Advances in Water*

30 *Resources , 51*, 280-291, 2013.

Seveno, F., Rodriguez, F., de Bondt K. and Joannis C.: Identification and representation of water pathways from production areas to urban catchment outlets: a case study in France, 2nd International Conference on the Design, Construction, Maintenance, Monitoring and Control of Urban Water, Germany, 2014.

Tang, T.; Reed, P.; Wagener, T. and Van Werkhoven, K.: Comparing sensitivity analysis methods to advance lumped watershed model identification and evaluation. *Hydrology and Earth System Sciences Discussions, 3*, 3333-3395, 2006.

Table 1: Summary of basin characteristics for both the Rezé and Pin Sec catchments

Description		Rezé	Pin Sec
Surface area		4.7 ha	31.3 ha
Housing type		Residential (individual)	Residential (individual and multi)
Mean building height (H$_{mean}$)		5.9 m	9.3 m
Land use	garden	55%	49%
	building	17%	19%
	road	28%	32%
Soil texture	clay	40%	8%
	sand	38%	51%
Imperviousness of the surface area		45%	51%
Impervious surfaces connected to the sewer		84%	61%
Length of sewer network	wastewater	803 m	3,911 m
	storm drain	480 m	6,972 m
Mean sewer depth		1.50 m	1.50 m

Table 2: Description of the hydrological parameters of the TEB-Hydro model as well as its MIN, MAX and REF values for the sensitivity analysis

Simulation	Parameter	Description	Unit	Values MIN	Values REF	Values MAX
SROAD	$W_{max,rd}^{surf}$	Maximum retention capacity of the road surface reservoir	mm	0.5	3.0	6.0
SROOF	$W_{max,rf}^{surf}$	Maximum retention capacity of the roof surface reservoir	mm	0.25	1.5	3.0
IP	I_p	Parameter that describes the water-tightness of the sewer pipe	-	10^{-3}	10^{-1}	1
IROAD	I_{rd}	Infiltration rate through the road	mm s^{-1}	10^{-9}	10^{-6}	10^{-5}
CONN	f_{con}	Fraction of impervious surfaces connected to the sewer network	-	0.5	0.7	0.9
DRAIN	D_*	Deep drainage	%	0	5	10

Figure 1: Schema of the hydrological processes involved in the TEB-Hydro model; subscripts *rf* and *bld* stand for building compartment, *rd* for road compartment, and *gdn* for garden compartment
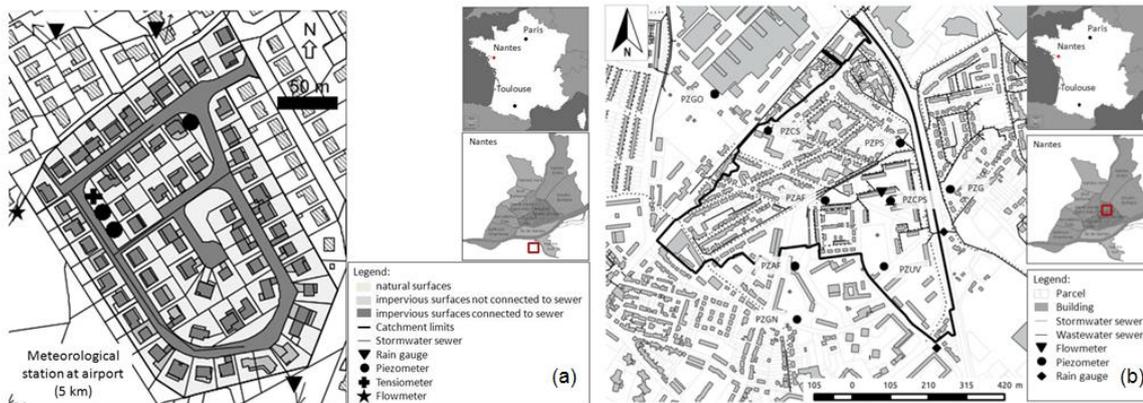
Figure 2: a) the experimental Rezé site (from Dupont, 2001); b) the experimental Pin Sec site. Maps to the right of the catchments indicate the location of Nantes (France) above and the Rezé and Pin Sec catchment locations (red square) in Nantes (middle)
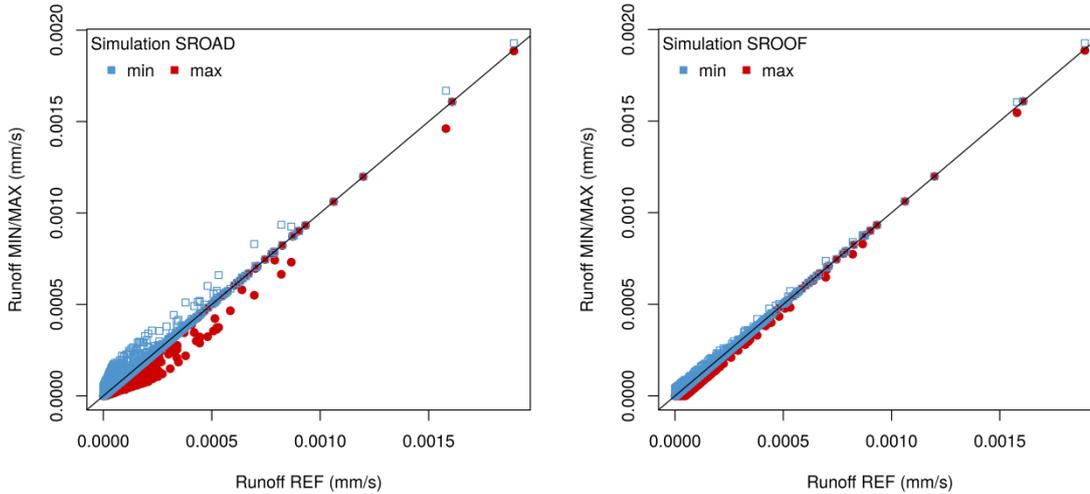
Figure 3: Comparison of urban runoff (R_{town}) between the reference simulation (REF) and both the MIN simulation (shown in blue) and MAX simulation (red) for the parameters: a) $W_{max,rd}^{surf}$ (left side), and b) $W_{max,rf}^{surf}$ (right side).
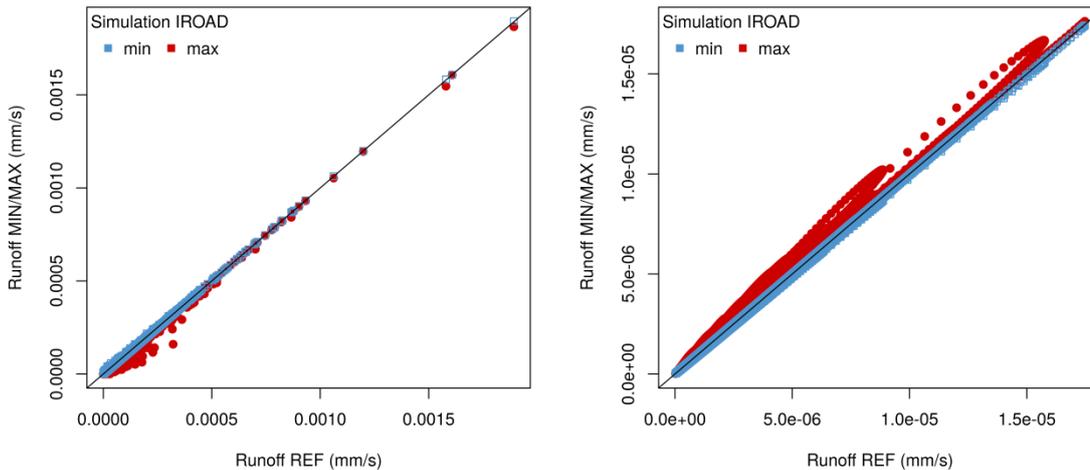
Figure 4: a) Comparison of urban runoff (R_{town}) between the reference simulation (REF) and both the MIN simulation (blue) and MAX simulation (red) for parameter I_{rd} on the left side; and b) comparison of the sewer runoff due to soil water infiltration (R_{sew}) between the reference simulation (REF) and the MIN (blue) and MAX (red) simulations for parameter I_{rd} on the right side
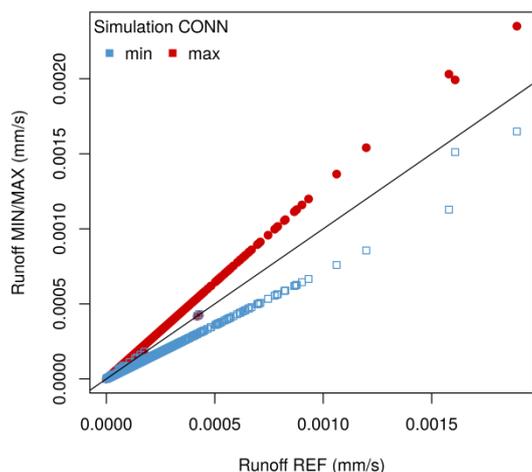
Figure 5: Comparison of urban runoff (R_{town}) between the reference simulation (REF) and the MIN (blue) and MAX (red) simulations for parameter f_{con}
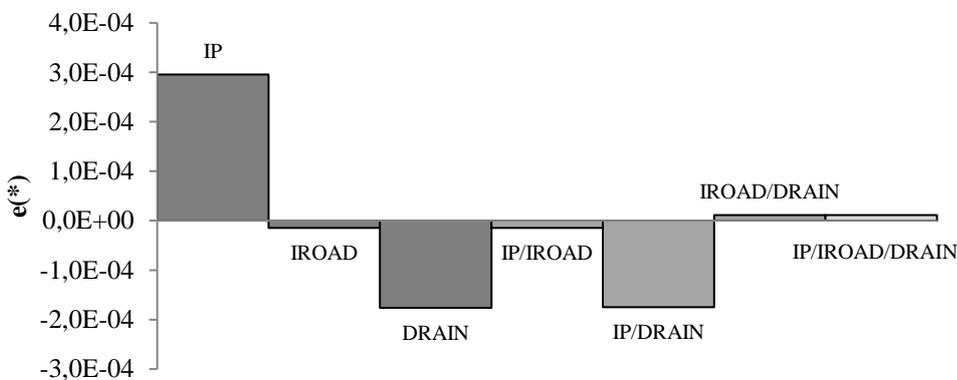
Figure 6: Calculated effects on the model response (R_{sew}) of parameters I_p, I_{rd} and D_* and their interactions. (dark shade of grey: principal effects, middle grey: second-order effects, and light grey: third-order effects)
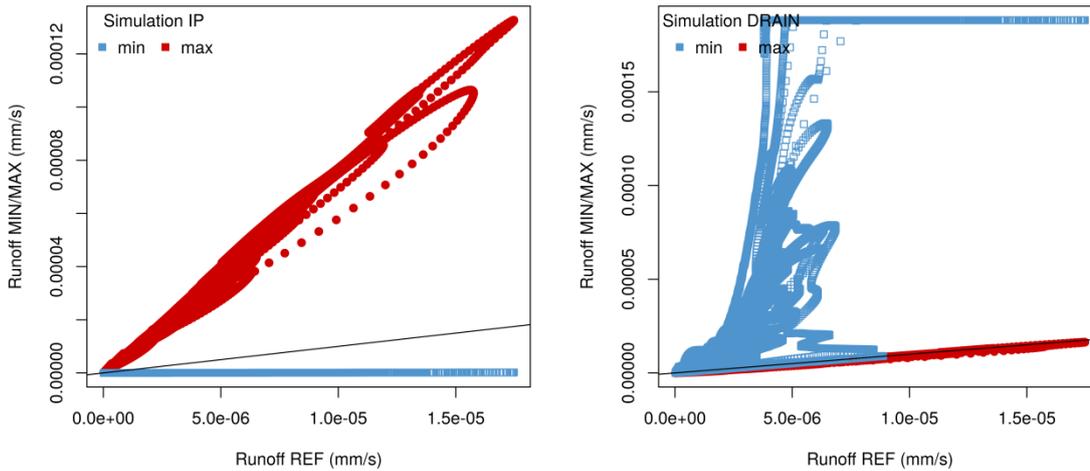
Figure 7: Comparison of sewer runoff due to soil water infiltration (R_{sew}) between the reference simulation (REF) and the MIN (blue) and MAX (red) simulations for parameters a) I_p (left side) and b) D_* (right side)
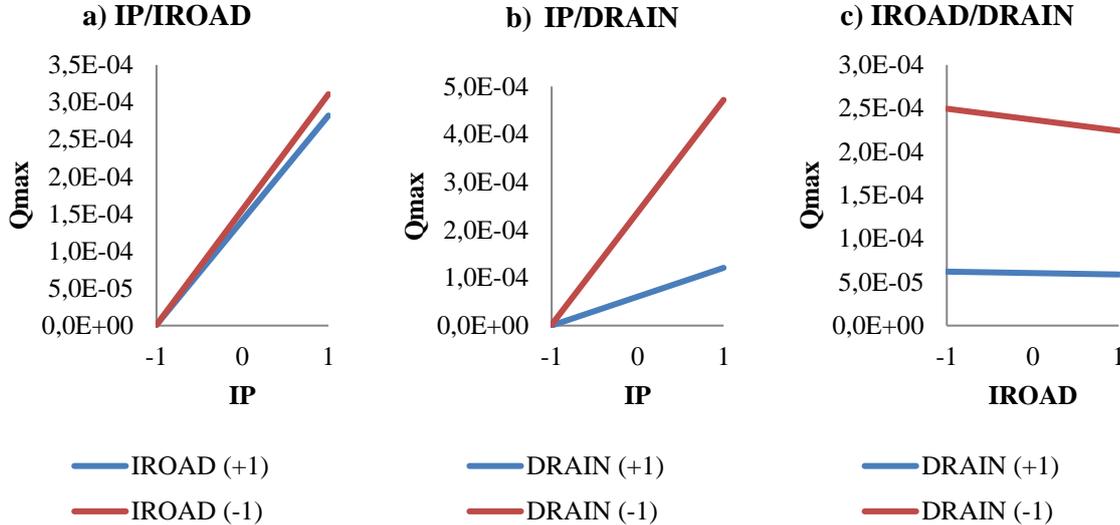
5   **Figure 8: Interactions as a function of the maximum observed sewer runoff due to soil water infiltration during winter 1994-95 of the second order between parameters: a) I_p and I_{rd}; b) I_p and D_* and of third order between parameters c) I_p, I_{rd} and D_***
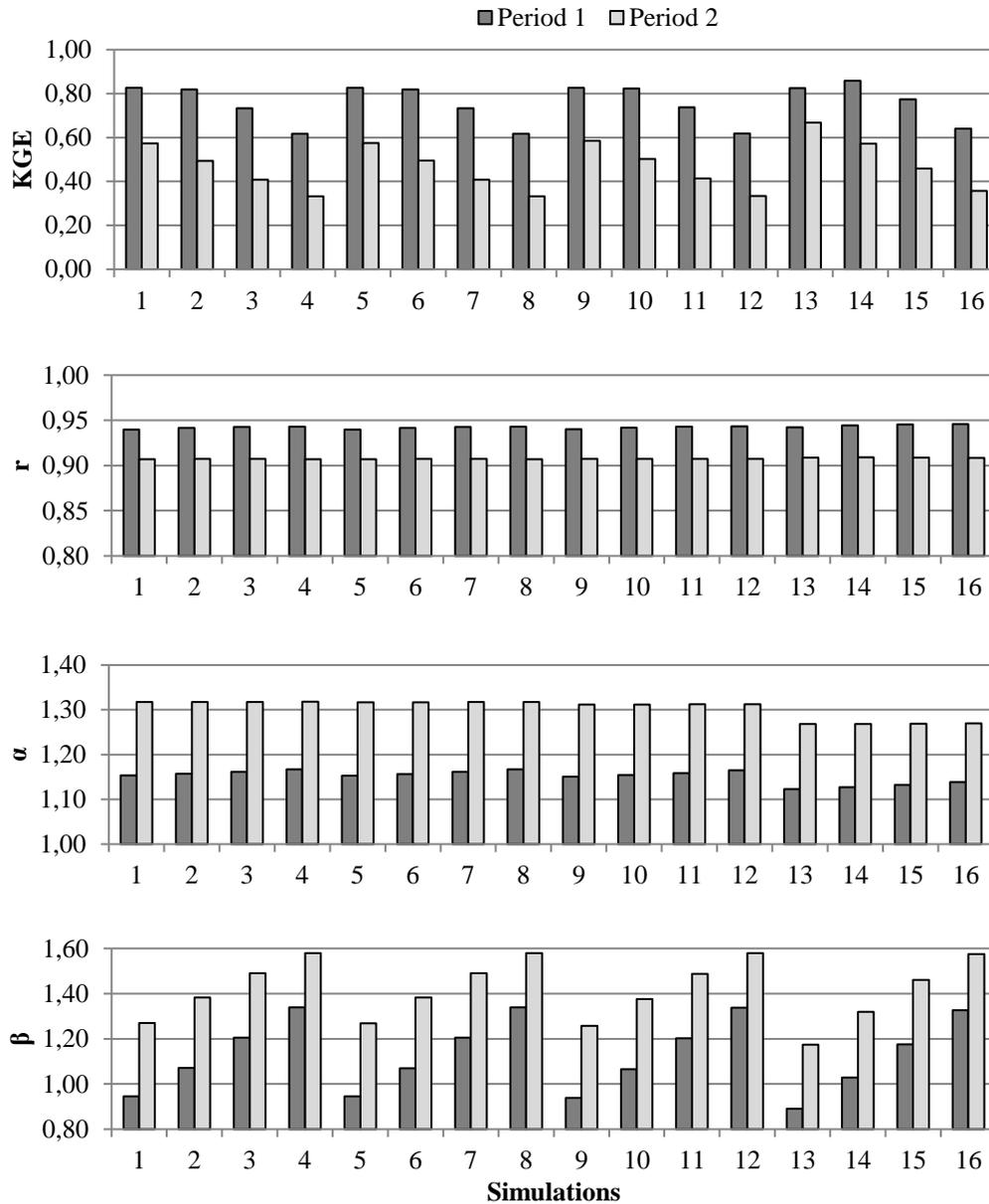
Simulations	1	2	3	4	5	6	7	8	9	10	11	12	13	14	15	16
I_p	0.09	0.3	0.6	1	0.09	0.3	0.6	1	0.09	0.3	0.6	1	0.09	0.3	0.6	1
I_{rd}	10^{-8}	10^{-8}	10^{-8}	10^{-8}	10^{-7}	10^{-7}	10^{-7}	10^{-7}	10^{-6}	10^{-6}	10^{-6}	10^{-6}	10^{-5}	10^{-5}	10^{-5}	10^{-5}
D_*	2	2	2	2	2	2	2	2	2	2	2	2	2	2	2	2

5   **Figure 9: Example of a calculated criterion for the simulation configurations where parameter D_* (deep drainage) is limited to 2% and all other parameters allowed to vary. The KGE criterion, the correlation criterion (r), the variability criterion (α) and the bias (β) for all 16 simulations and for the first (dark grey) and second (light grey) simulation periods are shown.**
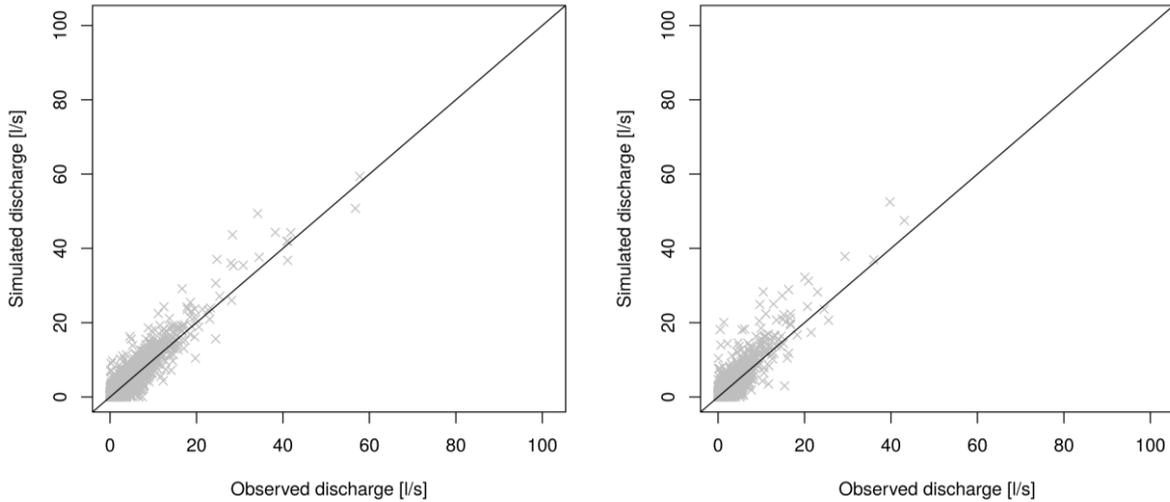
Figure 10: Comparison of simulated and observed total sewer discharge [l s⁻¹] during: a) the first simulation period from September 1993 to August 1995 (left side); and b) the second simulation period from September 1995 to August 1997 (right side) for Simulation 13 and a deep drainage limited to 2%
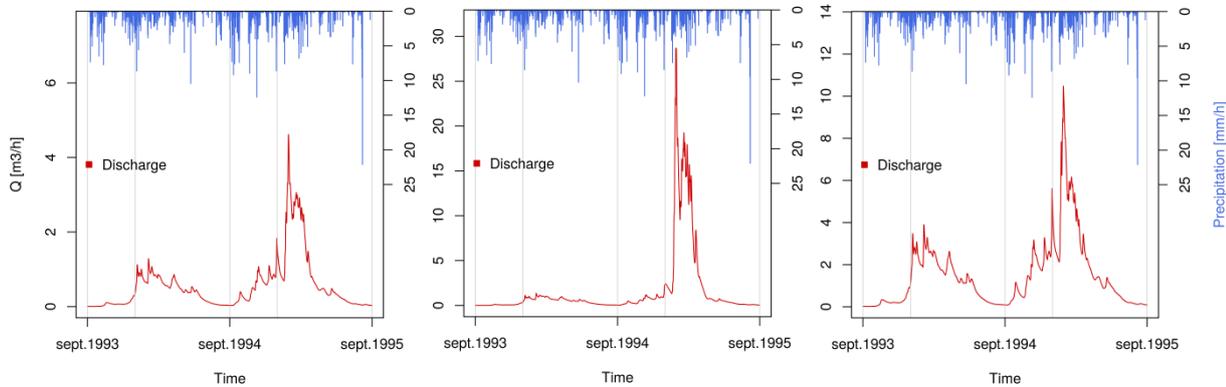
Figure 11: Simulated sewer discharge due to soil water infiltration during the first simulation period 1993-95 based on the combination of parameters I_p set at 0.09 and I_{rd} set at 10^{-5} and: a) D_* limited to 2%, b) D_* limited to 1%, and c) based on the combination of parameters I_p set at 0.3, I_{rd} set at 10^{-5}, with D_* limited to 2%